71

PROOF COPY [LF9295BJ] 055403PRB

Hofstadter-type spectral diagrams for the Bloch electron in three dimensions

J. Brüning,[1] V. V. Demidov,[2] and V. A. Geyler[2]

[1]*Mathematisch-Naturwissenschaftliche Fakultät II der Humboldt-Universität zu Berlin, Rudower Chaussee 25, Berlin 12489, Germany*

[2]*Laboratory of Mathematical Physics, Mordovian State University, Saransk 430000, Russia*

(Received 20 October 2003)

Flux-energy and angle-energy diagrams for an exact three-dimensional Hamiltonian of the Bloch electron in a uniform magnetic field are analyzed. The dependence of the structure of the diagrams on the direction of the field, the geometry of the Bravais lattice, and the number of atoms in an elementary cell is considered. Numerical evidence is given to show that the angle-energy diagram may have a fractal structure even in the case of a cubic lattice. It is shown that neglecting coupling of Landau bands changes considerably the shape of the diagrams. The Hall conductivity corresponding to the lowest Landau band is briefly discussed.

DOI: 10.1103/PhysRevB.69.0332XX PACS number(s): 71.15.Dx, 72.20.My, 73.43.−f, 73.22.−f

The spectral properties of an electron in a two-dimensional (2D) periodic structure with the Bravais lattice Λ in the presence of a uniform magnetic field $\mathbf{B}$ are determined by commensurability or noncommensurability of two geometric parameters: the area S of an elementary cell of Λ and the square of the magnetic length $l_M^2=\hbar/\mu\omega$ (here μ is the mass of the electron and ω is the cyclotron frequency). If $S/2\pi l_M^2$ is a rational number, then the electron energy spectrum has band structure, otherwise the spectrum is a fractal set. As a result, the flux-energy diagram for the spectrum has a remarkable recursive structure predicted by Azbel' and numerically discovered by Hofstadter in the framework of the tight-binding approximation.[1] The essential point in the appearance of such a structure is the size quantization of the electron motion along the field direction; hence it seems likely that in 3D periodic systems, the fractal structure of the flux-energy diagram must disappear.[2] Surprisingly, it was shown recently in a series of papers[3] that a fractal structure is visible in the diagram depicting the dependence of the spectrum on the angle between the field $\mathbf{B}$ (with fixed strength B) and a fixed vector in Λ, if Λ is an *anisotropic rectangular* lattice. Moreover, a series of energy gaps as in Hofstadter's butterfly arise in the *isotropic* case unless $\mathbf{B}$ points in high-symmetry crystallographic directions.[4]

The tight-binding approximation method used in Refs. 1,3,4 is based on a series of considerable simplifications of the initial periodic Landau operator, which imposes severe limitations of the method. In particular, the models considered in Refs. 3 and 4 give no way to take into account the effects of the interaction between Landau levels, which have profound effects on the shape of flux-energy diagrams and on the accompanying integer quantum Hall conductivity.[5] Even without the consideration of the Landau band coupling, the flux-energy diagrams obtained for the periodic Landau operator differ considerably from those for the tight-binding model.[6] In this paper, we get rid of the restrictions imposed by the tight-binding approximation method and analyze the angle-energy and the flux-energy diagrams for the 3D Landau operator perturbed by periodic potentials of various geometries. To deal with an explicitly solvable model, we consider periodic perturbations represented as sums of short-range potentials; in the zero-range limit we get an explicit expression for the dispersion relations, which is very useful for the numerical analysis. Such potentials were already used in the context of spectral problems for a 3D magneto-Bloch electron.[7,8] In the 2D case, the flux-energy diagrams for zero-range potentials were considered in Ref. 9.

The Hamiltonian H being studied is the sum $H=H_0+V$, where

$$H_0=\frac{1}{2\mu}\left(\mathbf{p}-\frac{e}{c}\mathbf{A}(\mathbf{r})\right)^2 \tag{1}$$

is the Landau operator with the vector potential $\mathbf{A}(\mathbf{r})=\mathbf{B}\times\mathbf{r}/2$, and V is the potential of a crystal lattice Γ with the Bravais lattice Λ. Let K be the set of all nodes of Γ lying in an elementary cell of Λ, then V is represented in the form

$$V(\mathbf{r})=\sum_{\kappa\in \mathrm{K}}\sum_{\lambda\in\Lambda}V_\kappa(\mathbf{r}-\boldsymbol{\lambda}), \tag{2}$$

where $V_\kappa(\mathbf{r})$ is the confinement potential of the node $\boldsymbol{\kappa}$ which is supposed to be short range. More precisely, we choose $V_\kappa(\mathbf{r})=c_\kappa W(\mathbf{r}-\boldsymbol{\kappa})$, where $W(\mathbf{r})\sim 0$ outside a small sphere of radius R centered at zero, $\int W(\mathbf{r})\,d\mathbf{r}=1$, and the coupling constant c_κ is of order R. At the zero-range limit, $R\to 0$, the potential V_κ is characterized by one parameter only, namely, by the scattering length ρ_κ, which is related to the binding energy of the ground state for V_κ by $E_\kappa=-\hbar^2/2\mu\rho_\kappa^2$.[10] Moreover, at this limit the Green function G of H, $G(\mathbf{r},\mathbf{r}';E)=\langle\mathbf{r}|(E-H)^{-1}|\mathbf{r}'\rangle$, has the following explicit expression in terms of the Green function $G_0(\mathbf{r},\mathbf{r}';E)$ of H_0.[10,11]:

$$G(\mathbf{r},\mathbf{r}';E)=G_0(\mathbf{r},\mathbf{r}';E)-\sum_{\gamma,\gamma'\in\Gamma}G_0(\mathbf{r},\gamma,E)\times[Q^{-1}(E)]_{\gamma,\gamma'}G_0(\gamma',\mathbf{r}';E). \tag{3}$$

Here $Q^{-1}(E)$ is the matrix inverse to the infinite matrix $Q(E)$ with elements

$$Q_{\gamma,\gamma'}(E)=\left[G_0^{\mathrm{ren}}(\gamma,\gamma,E)-\frac{\mu}{2\pi\hbar^2\rho_\gamma}\right]\delta_{\gamma,\gamma'}+(1-\delta_{\gamma,\gamma'})G_0(\gamma,\gamma';E), \tag{4}$$

PROOF COPY [LF9295BJ] 055403PRB

where G_0^{ren} denotes the renormalization of the unperturbed Green function G_0:

$$G_0^{\mathrm{ren}}(\mathbf{r},\mathbf{r}';E)=G_0(\mathbf{r},\mathbf{r}';E)-\frac{\mu}{2\pi\hbar^2}\frac{\exp[-i\pi\mathbf{b}(\mathbf{r}\times\mathbf{r}')]}{|\mathbf{r}-\mathbf{r}'|},$$

with $\mathbf{b}=\mathbf{B}e/2\pi\hbar c$ (note that $\phi_0=2\pi\hbar c/e$ is the magnetic flux quantum, therefore $\mathbf{b}$ is the density of the magnetic flux). The explicit form of G_0 is well known[11,12]

$$G_0(\mathbf{r},\mathbf{r}';E)$$
$$=\frac{\mu}{2^{3/2}\pi\hbar^2 l_M}\exp\left[-\pi i\mathbf{b}(\mathbf{r}\times\mathbf{r}')-\frac{(\mathbf{r}_\perp-\mathbf{r}'_\perp)^2}{4l_M^2}\right]$$
$$\times\sum_{l=0}^{\infty}\frac{\exp[-\sqrt{2(\varepsilon_l-E)/\hbar\omega}|\mathbf{r}_{\|}|/l_M]}{\sqrt{(\varepsilon_l-E)/\hbar\omega}}L_l(\mathbf{r}_\perp^2/2l_M^2). \tag{5}$$

Here $\mathbf{r}_{\|}$ is the projection of $\mathbf{r}$ on the direction of the field $\mathbf{B}$, $\mathbf{r}_\perp=\mathbf{r}-\mathbf{r}_{\|}$, $L_l(x)$ denotes the lth Laguerre polynomial, and $\varepsilon_l=\hbar\omega(l+1/2)$. Therefore, for all $\mathbf{r}$

$$G_0^{\mathrm{ren}}(\mathbf{r},\mathbf{r};E)=\frac{\mu}{2^{3/2}\pi\hbar^2 l_M}\zeta\left(\frac{1}{2},\frac{1}{2}-\frac{E}{\hbar\omega}\right), \tag{6}$$

where $\zeta(s,v)$ is the Hurwitz ζ function.[13]

It is clear that at least for $E<\hbar\omega/2$ the energy E belongs to the spectrum of H if the matrix $Q(E)$ is not invertible. Using the irreducible representations of the magnetic translation group (MTG) for H,[14] the problem to invert the infinite matrix $Q(E)$ may be reduced to a problem of finite-dimensional algebra. This reduction requires the so-called "rationality condition:" the field $\mathbf{B}$ is said to be *rational* with respect to the lattice Λ, if for a basis $\mathbf{a}_1$, $\mathbf{a}_2$, $\mathbf{a}_3$ of Λ, the numbers $\mathbf{b}(\mathbf{a}_j\times\mathbf{a}_k)$ are rational.[14] In this case a basis $\mathbf{a}_j$ ($j=1,2,3$) can be chosen in such a way that $\eta\equiv\mathbf{b}(\mathbf{a}_1\times\mathbf{a}_2)>0$ and $\mathbf{b}(\mathbf{a}_2\times\mathbf{a}_3)=\mathbf{b}(\mathbf{a}_1\times\mathbf{a}_3)=0$. Let $\eta=N/M$, where N and M are coprime positive integers. Then all the irreducible representations of the MTG which are trivial on the center of the group are M dimensional and are parametrized by a 3D torus $\mathbf{T}$.[14] It is convenient to choose coordinates of a point $\mathbf{p}$ from $\mathbf{T}$ such that $0\leqslant p_1<M^{-1}$, $0\leqslant p_2,p_3<1$. Then we can form the following $(MK)\times(MK)$ matrix $\tilde{Q}$, where K is the number of nodes in K:

$$\tilde{Q}_{q,q'}(\mathbf{p},E)$$
$$=\exp[-\pi i m'\mathbf{b}(\boldsymbol{\kappa}'\times\mathbf{a}_2)]$$
$$\times\sum_{\lambda_1,\lambda_2,\lambda_3=-\infty}^{\infty}\exp(-\pi i[2\boldsymbol{\lambda}\cdot\mathbf{p}+\eta\lambda_1(M\lambda_2+m)])$$
$$\times Q[\lambda_1\mathbf{a}_1+(\lambda_2 M+m)\mathbf{a}_2+\boldsymbol{\kappa},m'\mathbf{a}_2+\boldsymbol{\kappa}',\lambda_3\mathbf{a}_3;E]$$
$$\times\exp(\pi i[\lambda_1\mathbf{a}_1+(\lambda_2 M+m)\mathbf{a}_2](\mathbf{b}\times\boldsymbol{\kappa})). \tag{7}$$

Here q denotes the pair $(m,\boldsymbol{\kappa})$ with $\boldsymbol{\kappa}\in$ K, $m=0,\ldots,M-1$. Now the dispersion relation for H reads

$$\det\tilde{Q}(\mathbf{p},E)=0. \tag{8}$$

Equation (8) has for fixed $\mathbf{p}$ infinitely many solutions $E_s(\mathbf{p})$ (dispersion laws), which are continuous with respect to $\mathbf{p}$; each eigenvalue $E_s(\mathbf{p})$ is M-fold degenerate. By definition, the magnetic miniband J_s is the set of all values of $E_s(\mathbf{p})$. The minibands J_s lying below $\hbar\omega/2$ form a piece of the spectrum of H which may be attributed to broadening the ground state of H_0; therefore, this piece is nothing but the *lowest Landau band.* According to Eqs. (7) and (8), this band consists of KM magnetic minibands which can overlap. If the overlapping is absent, then the lowest Landau band approaches a Cantor set as M tends to infinity.

Using Eqs. (7) and (8) we analyze numerically the structure of the lowest Landau band for various types of crystal lattices and ranges of the field $\mathbf{B}$ employing two ways to force M to tend to infinity: (1) we change the value of B keeping the direction of $\mathbf{B}$ fixed; (2) we change the direction of $\mathbf{B}$ keeping the value of B fixed. The lattice constant $a=7.5$ nm is chosen relevant to the geometric parameters for the 3D regimented quantum dot superlattice considered recently in Ref. 15. As to the scattering length, we put $\rho\sim1$ nm, this corresponds to the binding energy $E\sim30$ meV.

The flux-energy diagrams for the simple-cubic lattice under various directions of $\mathbf{B}$ are depicted in Fig. 1 (here $\rho=2.5$ nm). If the magnetic field is directed along an edge of the cubic elementary cell, then all subbands overlap and the gaps are absent [Fig. 1(a)]. If the symmetry of the magnetic field with respect to the lattice decreases, then the number of open gaps increases and has tendency to infinite magnification [Figs. 1(b) and 1(c)] in full agreement with Ref. 4. Figure 2 shows the angle-energy diagrams for the lattice with the same geometric parameters and $\rho=1.1$ nm (in Figs. 2–4 $|\mathbf{b}|a^2=1$; for $a=7.5$ nm this corresponds to the field strength ~70 T). If the vector $\mathbf{B}$ is rotated inside a face of a cubic elementary cell, then the gaps, in general, overlap and the diagram reveals no fractal structure [Fig. 2(a)]. On the other hand, if the rotation plane forms a dihedral angle $\varphi=\arctan(3/4)$ with the plane of the face, then the fractal structure of the diagram is clearly visible [Fig. 2(b)]. Therefore, the condition of anisotropy[3] is not necessary for the appearance of a fractal structure in the angle-energy diagram. This can be understood taking the limit $B\to\infty$ in the matrix Q. Equation (4) shows that in this limit Q approximates the matrix of the tight-binding Hamiltonian from Ref. 3 with *energy-depending* coefficients t_j, and this dependence leads to an anisotropy of the limiting matrix without any anisotropy of the crystal lattice.

If in the representation (5) we restrict ourselves only to the first term, then this projection of the Green function on the lowest Landau level models the system without interaction between Landau levels. The corresponding diagram is given in Fig. 2(c).

To compare our results to those from Ref. 3 we consider the angle-energy diagrams for the tetragonal monoatomic lat-

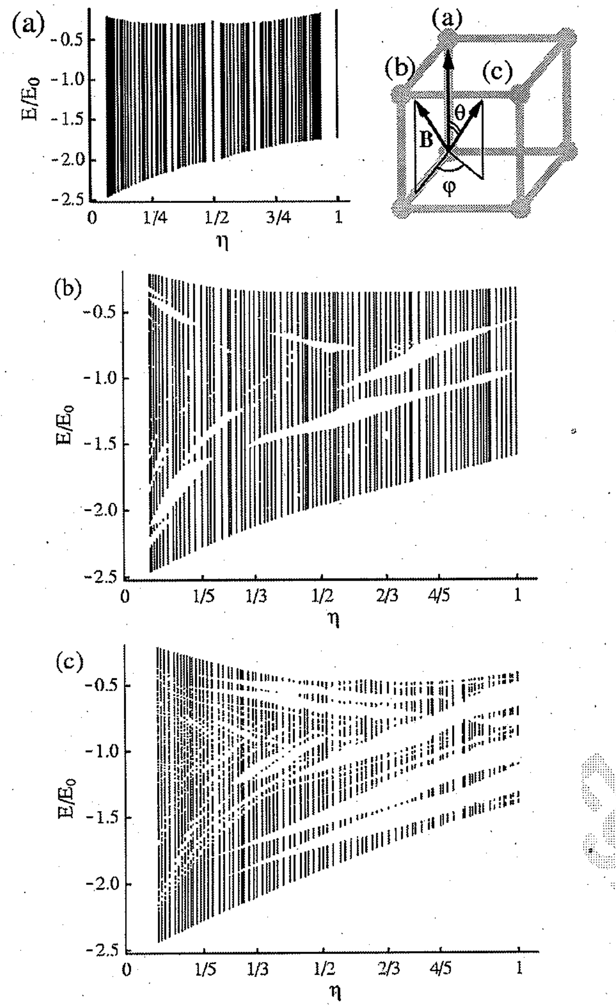

FIG. 1. The lowest Landau band of the simple-cubic lattice plotted against the magnetic flux for various directions of **B**: (a) $\mathbf{B}=(0,0,B)$; (b) $\mathbf{B}=(\frac{3}{5}B,0,\frac{4}{5}B)$; (c) $\mathbf{B}=(\frac{12}{25}B,\frac{9}{25}B,\frac{4}{5}B)$. Here and below $E_0=\hbar^2/\mu a^2$.

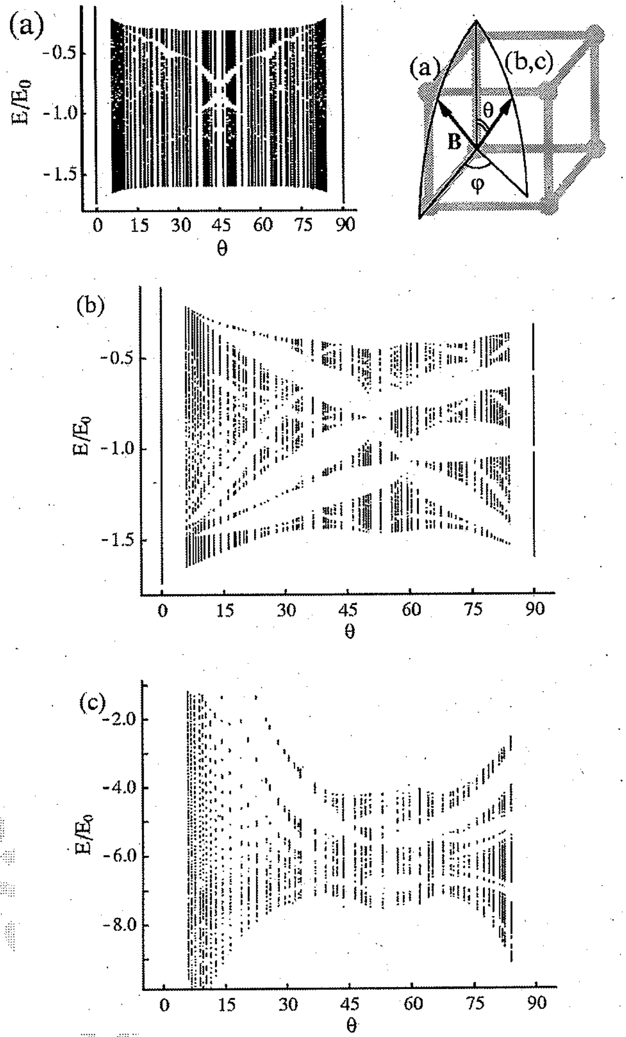

FIG. 2. The lowest Landau band of the simple-cubic lattice plotted against the tilting angle θ for various tilting orientations of **B**: (a) $\mathbf{B}=B(\sin\theta,0,\cos\theta)$; (b,c) $\mathbf{B}=B(\frac{4}{5}\sin\theta,\frac{3}{5}\sin\theta,\cos\theta)$, in panel (c) coupling between Landau levels is neglected.

tice with $\rho_0=2.5$ nm (Fig. 3). If the vector **B** is rotated in a face of an rectangular elementary cell, then we see a typical 1D-like energy spectrum in full agreement with Ref. 3. It is interesting that the *chemical anisotropy* radically transforms the shape of the angle-energy diagram. To show this, we consider a tetragonal double-atomic lattice with two sorts of atoms in an elementary cell with scattering lengths $\rho_1=2.5$ nm and $\rho_2=0.6$ nm (Fig. 4). If **B** is rotated in a face of anisotropy, then the angle-energy diagram looks like deformed Hofstadter's butterfly. Since in this case $K=2$, there is a doubling of minibands that causes the appearance of a wide gap in the diagram ("atomic" gap). On the other hand, if **B** rotates in the plane perpendicular to the anisotropy axis, only the atomic gap appears in the diagram. (Figure 4(a) arises from Fig. 2(a) by the doubling of all bands).

As a conclusion, we have derived a dispersion relation for a 3D Bloch electron in a uniform magnetic field [Eqs. (7) and (8)] and analyzed the corresponding flux-energy and angle-energy diagrams. For anisotropic rectangular crystals we confirm the results of Refs. 3 and 4 concerning the structure of these diagrams. Moreover, we show that the anisotropy is not necessary for the appearance of a multitude of gaps both in flux-energy and angle-energy diagrams. Neglecting coupling of Landau bands leads to a substantial deformation of angle-energy diagram. Chemical anisotropy of the considered crystal (the presence of distinct sorts of atoms in an elementary cell of the Bravais lattice) leads to another deformation of the diagram, in particular, to the appearance of an additional wide gap.

Let us discuss briefly the Hall conductance σ_{jk}, $j,k=x,y,z$, $j\neq k$. According to the Kohmoto-Halperin-Wu formula,[16] at the Fermi energy E_F, lying in a gap, $\sigma_{jk}(E_F)$ equals (up to the factor $-e^2/h$) to the corresponding Chern number of the magneto-Bloch vector bundle associated with E_F. These numbers can be found with the help of Eqs. (7)

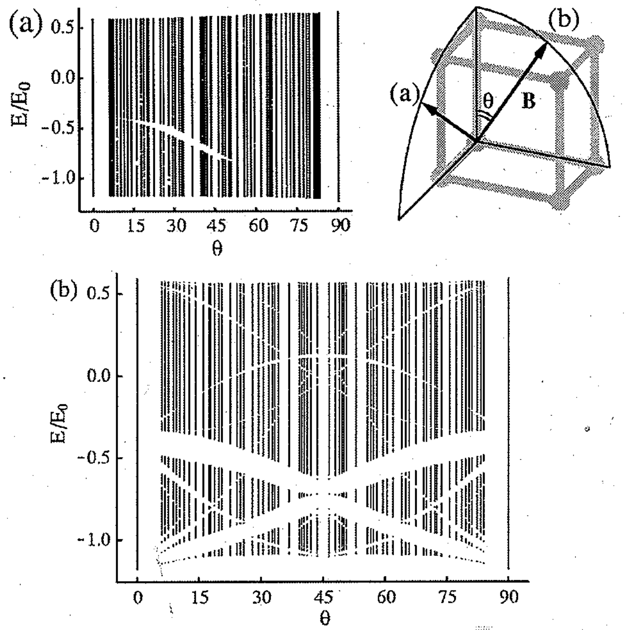

FIG. 3. The lowest Landau band of the tetragonal monoatomic lattice [with lattice constants $(a/2,a,a)$] plotted against the tilting angle θ for various tilting orientations of **B**: (a) $\mathbf{B}=B(\sin\theta,0,\cos\theta)$; (b) $\mathbf{B}=B(0,\sin\theta,\cos\theta)$.

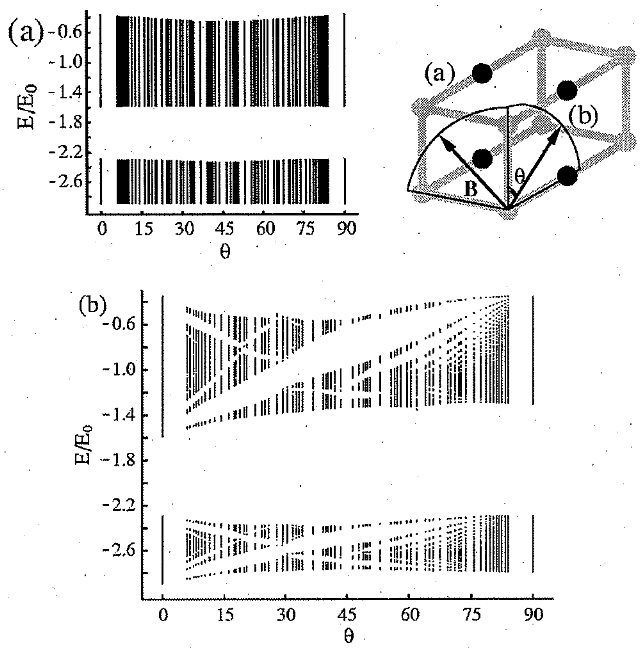

FIG. 4. The lowest Landau band of the tetragonal double-atomic lattice [with lattice constants $(2a,a,a)$] plotted against the tilting angle θ for various tilting orientations of **B**: (a) $\mathbf{B}=B(0,\sin\theta,\cos\theta)$; (b) $\mathbf{B}=B(\sin\theta,0,\cos\theta)$.

and (8). We mention here only the following strict result: *The Hall conductance $\sigma_{jk}(E_F)$ corresponding to the entirely filled lowest Landau band vanishes* [but for the subbands $\sigma_{jk}(E_F)$ are, in generical, nonzero integers]. In 2D case, such a phenomenon was observed in Ref. 17.

The work is partially supported by DFG SFB-288 "Differentialgeometrie und Quantenphysik" and by Grants of DFG–RAS (Grant No. 113/572/0-2), INTAS (Grant No. 00-257), and RFBR (Grant No. 02-01-00804).

[1] M.Ya. Azbel', Sov. Phys. JETP **46**, 634 (1964); D. Hofstadter, Phys. Rev. B **14**, 2239 (1976).
[2] Y. Hasegava, J. Phys. Soc. Jpn. **59**, 4384 (1990); Z. Kunszt and A. Zee, Phys. Rev. B **44**, 6842 (1991).
[3] M. Koshino, H. Aoki, T. Osada, K. Kuroki, and S. Kagoshima, Phys. Rev. Lett. **86**, 1062 (2001); Phys. Rev. B **65**, 045310 (2002); M. Koshino, H. Aoki, and B.I. Halperin, *ibid.* **66**, 081301 (2002).
[4] M. Koshino and H. Aoki, Phys. Rev. B **67**, 195336 (2003).
[5] O. Kühn, P.E. Selbmann, V. Fessatidis, and H.L. Cui, J. Phys.: Condens. Matter **5**, 8225 (1993); D. Springsguth, R. Ketzmerick, and T. Geisel, Phys. Rev. B **56**, 2036 (1997).
[6] G. Petschel and T. Geisel, Phys. Rev. Lett. **71**, 239 (1993); O. Kühn, V. Fessatidis, H.L. Cui, P.E. Selbmann, and N.J.M. Horing, Phys. Rev. B **47**, 13 019 (1993).
[7] V.A. Geyler and V.A. Margulis, Sov. Phys. JETP **68**, 654 (1989); Y. Avishai, M.Ya. Azbel', and S.A. Gredeskul, Phys. Rev. B **48**, 17 280 (1993).
[8] V.A. Geyler and V.V. Demidov, Theor. Math. Phys. **103**, 561 (1995).
[9] S.A. Gredeskul, M. Zusman, Y. Avishai, and M.Ya. Azbel', Phys. Rep. **288**, 223 (1997); V.A. Geyler, I.Yu. Popov, A.V. Popov, and A.A. Ovechkina, Chaos, Solitons Fractals **11**, 281 (2000).
[10] Yu.N. Demkov and V.N. Ostrovskiy, *Zero-Range Potentials and Their Applications in Atomic Physics* (Plenum Press, New York, 1988); S. Albeverio, F. Gesztesy, R. Høegh-Krohn, and H. Holden, *Solvable Models in Quantum Mechanics* (Springer-Verlag, Berlin, 1988).
[11] V.A. Geyler and V.A. Margulis, Theor. Math. Phys. **70**, 133 (1987).
[12] G. Gountarulis, Phys. Lett. **36A**, 132 (1972).
[13] H. Bateman and A. Erdélyi, *Higher Transcendental Functions*, (McGraw-Hill, New York, 1953), Vol I.
[14] J. Zak, Phys. Rev. **134A**, 1607 (1964).
[15] O.L. Lazarenkova and A.A. Balandin, Phys. Rev. B **66**, 245319 (2002).
[16] M. Kohmoto, B.I. Halperin, and Y.S. Wu, Phys. Rev. B **45**, 13 488 (1992).
[17] Z. Tešanović, F. Axel, and B.I. Halperin, Phys. Rev. B **39**, 8525 (1989).